Unravelling the Mechanisms Behind Mixed Catalysts for the High Yield Production of Single-Walled Carbon Nanotubes

Sailaja Tetali,[†,‡] Mujtaba Zaka,[§] Ronny Schönfelder,[†] Alicja Bachmatiuk,[†] Felix Börrnert,[†] Imad Ibrahim,[†,‡] Jarrn H. Lin,[⊥] Gianaurelio Cuniberti,[‡] Jamie H. Warner,[§] Bernd Büchner,[†] and Mark H. Rümmeli[†,*]

[†]IFW Dresden, P.O. Box 270116, D-01171 Dresden, Germany, [‡]Institute for Materials Science and Max Bergmann Center of Biomaterials, Dresden University of Technology, D-01062 Dresden, Germany, [§]Department of Materials, University of Oxford, Parks Road, Oxford OX1 3PH, United Kingdom, and [⊥]Department of Material Science, National University of Tainan, 33, Sec. 2, Shu-Lin Street, Tainan, Taiwan 700, Republic of China

ABSTRACT The use of mixed catalysts for the high-yield production of single-walled carbon nanotubes is well-known. The mechanisms behind the improved yield are poorly understood. In this study, we systematically explore different catalyst combinations from Ni, Co, and Mo for the synthesis of carbon nanotubes *via* laser evaporation. Our findings reveal that the mixing of catalysts alters the catalyst cluster size distribution, maximizing the clusters' potential to form a hemispherical cap at nucleation and, hence, form a single-walled carbon nanotube. This process significantly improves the single-walled carbon nanotube yields.

KEYWORDS: carbon nanotubes · mixed catalysts · growth mechanism · diameter and yield control

Modifying the arc-discharge process for the synthesis of carbon nanotubes by the inclusion of transition metals led to the discovery of single-walled carbon nanotube (SWNT) formation.[1] In the years that followed, several groups showed that the use of binary catalysts could significantly improve the yield. The earliest studies were conducted using the arc-discharge synthesis route; for example, Seraphin and Zhou[2] showed high yields of SWNT from Fe/Ni and Co/Ni catalysts. Journet *et al.* declared yields of up to 90% with Ni/Co, Ni/Y, and Co/Y mixes.[3] Saito *et al.* showed the potential of Pt/Rh mixes.[4] These investigations were complemented by laser ablation studies claiming yields up to 70% using Ni/Co mixes.[5] Indeed, Ni/Co became one of the more popular catalyst mixes. Within chemical vapor deposition (CVD), the synthesis of carbon nanotubes using mixed catalysts is also acclaimed for improved yield and vertically aligned carbon nanotubes. Some early works of note are the careful assessment of Fe/Mo catalyst mixes for mats of vertically aligned multiwalled carbon nanotubes (MWNT)[6] and vertically aligned mats of SWNT using Co/Mo.[7]

Despite the success of mixed catalysts for high-yield carbon nanotube synthesis, few studies on the role of mixed catalysts exist. Such investigations generally require systematic and patient evaluation not only through different catalyst mix ratios but also with the synthesis parameters. Unsurprisingly, most efforts are based on CVD because it is the most promising method for mass production and integration into silicon technology. However, in CVD, the role of the catalyst is argued to go beyond simply nucleating and growing the carbon nanotubes; the catalysts may also be actively involved in the catalytic decomposition of the hydrocarbon feedstock. For example, a study by Liao *et al.* investigated different Co−Mo compositions. They found the morphology of the carbon nanotube products to vary. With 5−15 atom % Co, they tended to produce long MWNTs, while with 40−50 atom % Co, they found short MWNTs. Higher amounts of Co led to structures with onionated morphology. They attributed this to the addition of Mo to Co reducing the CO decomposition rate and consequently the CNT length.[8] On the other hand, others suggest that the catalysts' role on the chemical decomposition process is not so important, but that altered melting points and modified carbon solubility in the catalyst nanoparticles are more important.[9] Lolli *et al.* showed that Co−Mo combinations result in smaller and more stable cluster sizes as compared to pure

*Address correspondence to m.ruemmeli@ifw-dresden.de.

Received for review September 19, 2009 and accepted October 30, 2009.

Published online November 2, 2009.
10.1021/nn9012548 CCC: $40.75

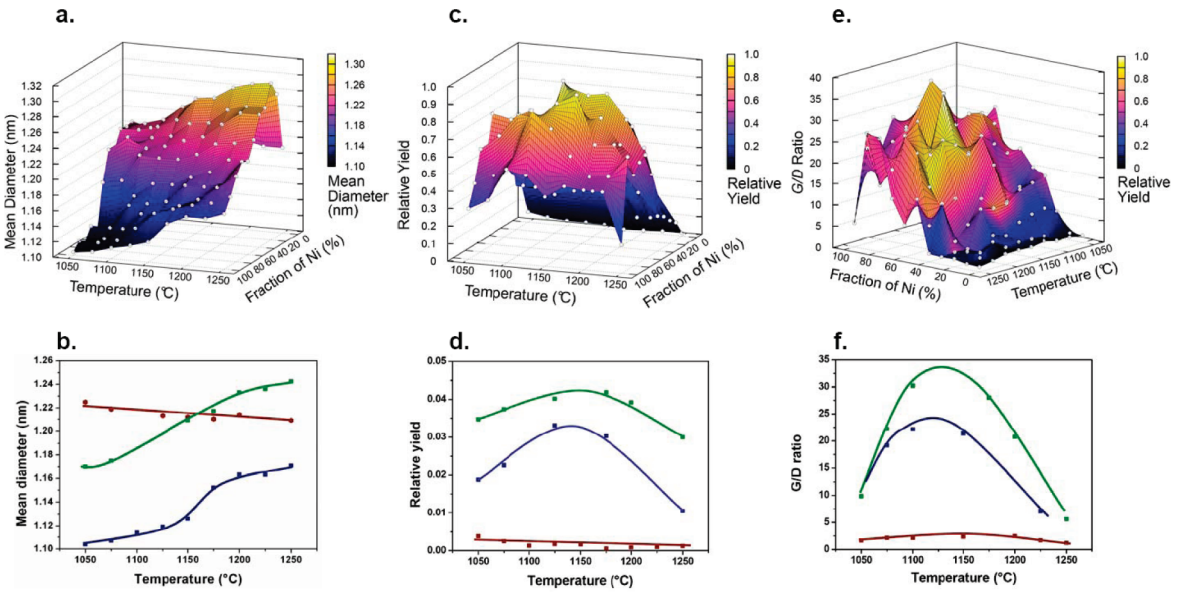

Figure 1. (a) Three-dimensional plot showing the mean diameter dependence on oven temperature and Ni/Co ratio. (b) Two-dimensional plot of mean diameter *vs* oven temperature for pure Ni (lower sigmoid curve), pure Co (linear curve), and Ni/Co (1:1) (upper sigmoid curve). (c) Three-dimensional plot of relative yield against oven temperature and Ni/Co ratio. (d) Two-dimensional plot of relative yield. From bottom up: pure Co, pure Ni, Ni/Co (1:1). (e) Four-dimensional plot of G/D ratio dependence on catalyst Ni/Co ratio and oven temperature. The shading corresponds to yield. (f) Two-dimensional plot illustrating the G/D change with temperature and catalyst ratio. From bottom up: pure Co, pure Ni, Ni/Co (1:1). Curves are a guide to the eye.

Co.[10] Thus, there remains a need to study mixed catalysts, particularly for non-CVD-based routes. In this study, we systematically investigate various catalyst mix systems involving Ni, Co, and Mo for the synthesis of SWNTs using laser evaporation. In laser evaporation, a graphite target containing catalyst material is evaporated in a reactor sitting at an elevated temperature within a buffer gas, such as argon or nitrogen. Hydrocarbon decomposition is therefore not involved, simplifying the study. In addition, the process parameters (*e.g.*, temperature, pressure, flow rate) are easily controlled, making laser evaporation an excellent platform to study carbon nanotube growth mechanisms.[11]

RESULTS

Transitions between van Hove singularities in SWNT led to distinctive interband absorption peaks in optical absorption spectroscopy (OAS) in the IR region of the electromagnetic spectrum. The two most intense peaks correspond to the first two transitions from semiconducting SWNTs and are referred to as the S_{11} and S_{22} peaks, while the third and weakest peak arises from metallic tubes and is termed the M_{11} peak. The background beneath the peaks corresponds to the π plasmon from carbonaceous species, *viz.* SWNT and amorphous carbon. Thus, the relative intensity of the peaks to the background provides a measure of the purity (SWNT to amorphous species).[12] Quantitative changes in purity between samples can be determined by normalizing the spectra and subtracting the background and examining the relative peak intensities. In addition, the peak widths correspond to the diameter distribution and can be used to determine the mean diameter.[12−14] These aspects are illustrated in Figure S1 in the Supporting Information. In these studies, the S_{11} peak was used. Corrections were made due to excitonic effects when extracting diameter information.[15]

Figure 1a shows a 3D graph of the mean diameter variation with oven temperature and Ni to Co ratio, from pure Ni through pure Co. With respect to temperature, the mean diameter shows a sigmoid shape from pure nickel, which gradually becomes less pronounced as the Co content increases such that, by the time the catalyst solely comprises Co, the variation with temperature is linear with a slightly negative slope. This temperature-dependent evolution is also highlighted in 2D in Figure 1b. For a given temperature, the mean diameter is at a minimum for pure Ni, which increases to a maximum as more Co is added to the mix. With large Co content (>80%), the mean diameter begins to fall. The maximum occurs with less relative Co content as temperature increases.

The OAS data also provide information on the relative yield of the samples, and in Figure 1c, a 3D plot of the relative yield *versus* temperature and Ni/Co content is plotted. With pure Ni as the catalyst, the yield shows a parabolic behavior with respect to temperature with a maximum around 1150−1175 °C. As greater amounts of Co are added to the mix, the parabolic profile begins to flatten and the maximum relative yield increases to a maximum for a Ni/Co ratio of 1. As more Co is added, the parabolic profile flattens considerably such that the profile is linear for a catalyst content consisting entirely of Co (see Figure 1d). The relative yields from high Co content catalysts (>80%) are very weak, even compared to pure Ni.

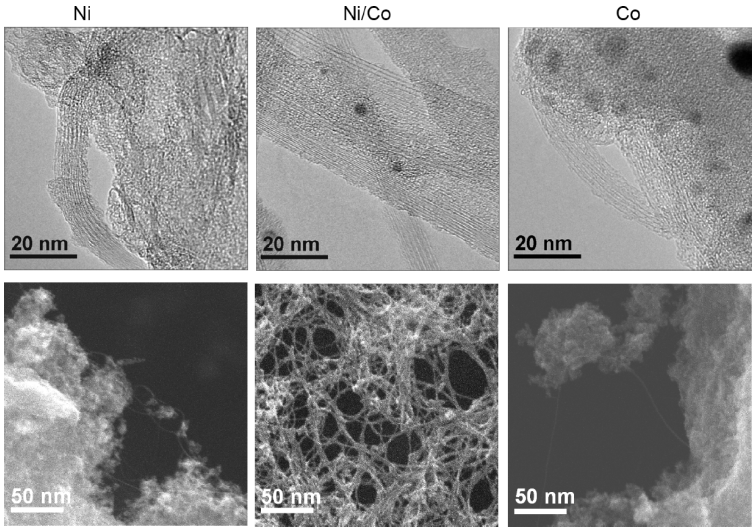

Figure 2. TEM (top row) and SEM (bottom row) from SWNT samples produced with Ni, Ni/Co (1:1), and Co catalysts at 1150 °C. The improved yield from the Ni/Co catalyst is apparent.

TEM and SEM studies confirm the change in yield through visible changes in the amount of amorphous species relative the SWNTs. In addition, as the yield increases (less amorphous carbon), the SWNT bundle sizes are seen to increase. Figure 2 provides microscopy examples highlighting changes in yield with catalyst.

Raman spectroscopy has been shown to be a perfect tool to evaluate the crystallinity in different sp^2-hybridized carbon structures. For SWNTs, a strong Raman-active tangential mode (G-line) is observed around 1590 cm^{-1}, and scattering on defects gives rise to a defect-induced mode (D-mode) around 1300 cm^{-1}. At lower frequencies, the diameter-dependent radial breathing modes (RBM) typical for SWNT are observable. An example Raman spectrum is provided in Figure S2 in the Supporting Information. For all of our samples, the spectral shape of the Raman response is similar. Changes in the RBM due to mean diameter shifts concomitant with the OAS data are observed (data not shown). In addition, relative changes between the G- and D-modes are found. The G/D ratio is often used as a measure of crystallinity. In Figure 1e,f, 4D and 2D plots, respectively, of the G/D ratio with temperature and catalyst Ni/Co content are shown. In panel e, the shading corresponds to the yield. The profile is very similar to the variation in sample yield (Figure 1c,d) and shows there is a strong synergy between the SWNT yield and their crystallinity.

In addition to exploring Ni/Co catalyst mixes, we also investigated Ni/Mo and Co/Mo mixes at a temperature of 1150 °C (Ni/Co optimum temperature). Figure 3a,b shows the variation of the mean diameter with decreasing Mo content and temperature for Ni and Co, respectively. For Ni/Mo catalyst mixes, the mean diameter tends to increase as the Mo content increases and also for temperature increase. In the case of Co/Mo, the changes in mean diameter are minor with the exception of high temperatures and a 90% Mo loading. In Figure 3c,d, the relative yields are presented for Ni/Mo and Co/Mo, respectively. In addition, the yields from pure Ni and pure Co are included for comparison. Relative to the pure metal (Ni or Co), the addition of Mo clearly enhances the yield. In the case of Ni, the addition of Mo approximately doubles the yield and does not exhibit strong changes with respect to the amount of Mo mixed in. The increase in yield when Mo is added to Co is greater and appears to be at a maximum with only small fractions of Mo. The yield then tends to decrease as the Mo loading increases. The maximum observed increase in yield is almost an order of magnitude for 10% Mo addition to Co.

The inclusion of Mo was also explored with different Ni/Co mixes at 1175 °C. The mean diameter and relative yield for the different Ni/Co/Mo catalyst mixtures synthesized at 1175 °C are presented in Figure 4a,b.

Only minor changes in the mean diameter are observed for the different Ni/Co/Mo ratios investigated. Changes in the yield are more obvious depending on the Ni/Co/Mo ratio. In addition, the relative yields are compared to equivalent Ni/Co ratios without Mo added.

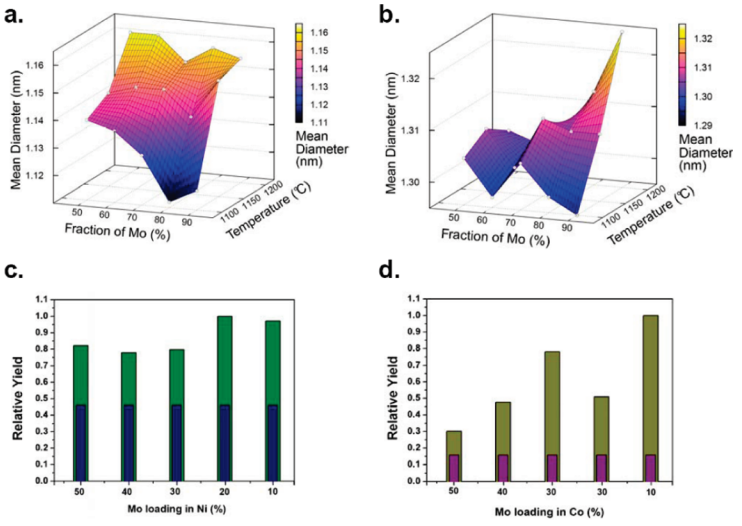

Figure 3. (a) Mean diameter dependence with temperature and (b) Mo loading for Ni and Co. (c,d) Relative yield *versus* Mo loading in Ni and Co, respectively, at 1150 °C. Inner (lower intensity) bars represent yield for pure Ni and Co, respectively.

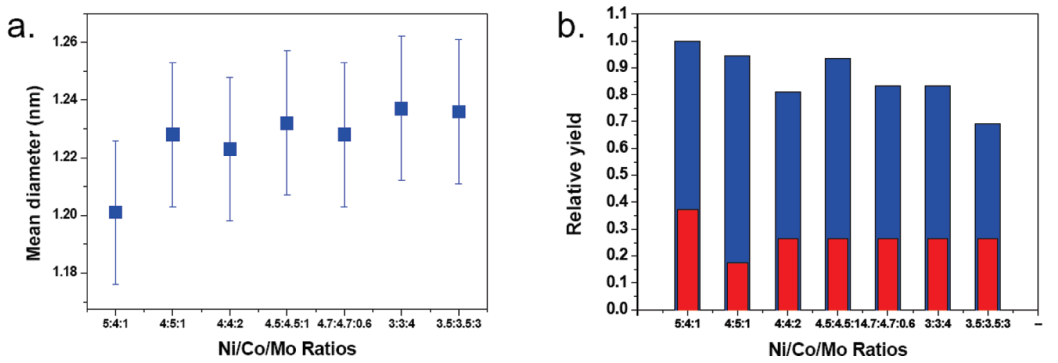

Figure 4. (a) Mean diameter for different Ni/Co/Mo ratios. Oven temperature = 1175 °C. (b) Relative yield for different Ni/Co/Mo ratios at 1175 °C (blue bars). The less intense bars (red) represent the yield from equivalent Ni/Co ratios without Mo with a reaction temperature of 1175 °C.

The inclusion of Mo increases the yield by a factor of 3 to 4.

From this study, it is clear that binary or ternary catalyst mixtures lead to higher yields as compared to single metal catalysts. In addition, Ni and Co as individual catalysts differ in their temperature dependence regardless of mean diameter and yield. To gain further insight into the mechanisms behind the increase in yield, we also looked at the SWNT diameter distribution changes with the catalyst mix. The diameter distribution, as mentioned above, can be obtained from the peak profiles in OAS. Previous studies of ours showed that, for a Pt/Rh/Re catalyst mix, the yield went through a maximum as one increased the temperature and that this is correlated with the diameter distribution of SWNTs.[11]

In this study, again a correlation with yield and SWNT diameter distribution is found. Figure 5a shows the full width at half-maximum (fwhm) of selected samples as derived from the S_{11} OAS peaks. The selected samples are all synthesized at 1150 °C, and the catalyst mixes were as follows: pure Ni, Ni/Mo (9:1), pure Co, Co/Mo (9:1), Ni/Co (1:1), and Ni/Co/Mo (5:4:1). The smallest fwhm is observed for Ni (*ca.* 0.18 nm), while the largest is observed for pure Co (*ca.* 0.32 nm). Remarkably, all of the mixed catalyst systems with enhanced yields relative to the pure metals exhibit similar fwhm values (*ca.* 0.22 nm). For comparison, the yield and the mean diameters for the samples are provided in panels b and c, respectively. From panel b, it is obvious the best yield is obtained with a combination of Ni, Co, and Mo. From panel c, one can discern that larger diameters are obtained if Co is present in the system. The largest diameter is obtained from Co/Mo catalysts.

DISCUSSION

The various data show one can tailor the mean diameter, diameter distribution, and yield of laser evaporated SWNTs through catalyst choice, mix ratio, and temperature. For most applications, it is desirable to produce samples with high yield. To this end, mixed catalyst systems are clearly superior to single metal catalysts.

Some of the observations found here are in agreement with previous studies of ours that investigated Pt/Rh/Re catalysts. Those studies focused on the temperature/mean diameter/yield dependence for a fixed catalyst ratio. In that study, the observations were all explained within a remarkably simple model, the so termed *catalyst volume to surface area* model. In this model, the amount of carbon precipitating from the catalyst particle at the point of nucleation depends (at a basic level) on the catalysts' volume for a given catalyst system (carbon solubility). In addition, it assumes that a hemispherical cap is required for nucleation, in agreement with Fan's density functional theory calculations[16] which show such caps are overwhelmingly preferred for SWNT nucleation. Hence, if insufficient carbon is available at the point the catalyst particles precipitate their carbon (due to cooling), no stable hemispherical cap forms. This makes the particle vulnerable to other process (*e.g.*, sintering) and is unlikely

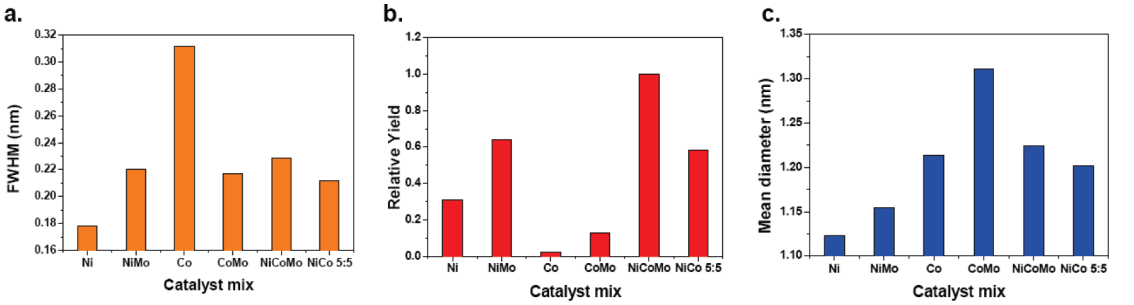

Figure 5. (a) Comparison of SWNT diameter distribution fwhm for pure Ni and Co against various catalyst mixes. (The fwhm is derived from the S_{11} peak from the absorption spectra.) (b) Relative yield and (c) mean diameter for the same catalyst mixes as in panel a.

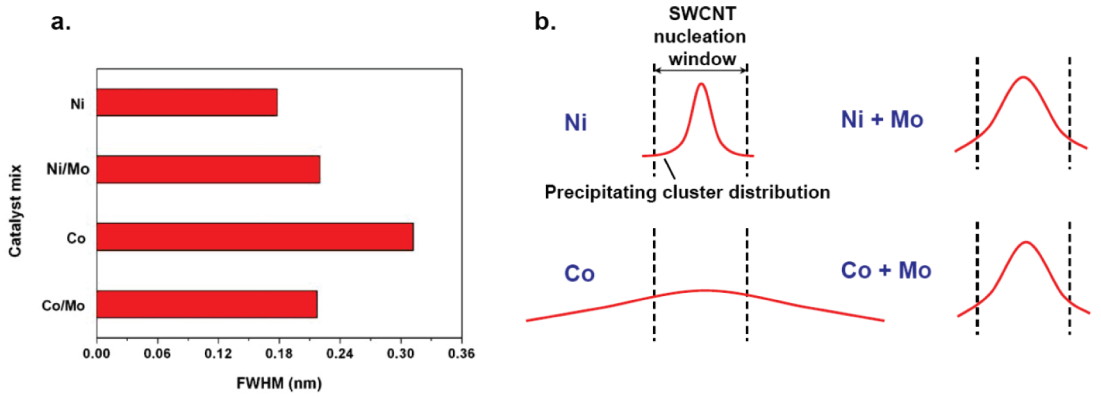

Figure 6. (a) SWNT diameter distribution changes (fwhm) for pure Ni and Co and Ni/Mo and Co/Mo (9:1 in both cases). (b) Schematic representing the change in precipitating cluster distribution relative to the nucleation window (hemispherical cap formation) for Ni and Co when adding Mo. In the case of Ni, the cluster size distribution expands, leading to higher yields. In the case of Co, the precipitating cluster distribution shrinks, again increasing the yield (*cf.* panel a).

to nucleate a SWNT. Increasing the catalyst size will lead to sufficient carbon being available to form a hemispherical cap due to the carbon supply being volume-dependent while the cap is area-dependent. SWNTs can then nucleate and grow. If the particle is too big, however, there is an excess of carbon that leads to the particle being encapsulated. Hence, due to the above stated catalyst volume to surface area restrictions, a SWNT nucleation cluster size window exists. Moreover, the catalyst cluster size distribution (at the point of nucleation) is independent of the nucleation cluster window. SWNTs only form when the nucleation cluster size window and precipitating cluster size distribution overlap. The precipitating cluster size shifts with temperature, and so one can control this overlap to tailor the mean diameter, SWNT size distribution, and yield according to the degree of overlap. Indeed, this is observed in the sigmoid dependence observed in the Ni- and Ni/Co-catalyzed samples (Figure 1). Initially, at lower temperatures, the overlap between the nucleation cluster size distribution and the precipitating cluster size distribution is minimal, and the mean diameter will be at its lowest. As the temperature increases, the overlap increases further and the mean diameter (and yield) increases slightly. Once the bulk of the precipitating cluster size distribution lies within the nucleation window, the yield will be at its highest, and as it shifts through the window, the change in mean diameter will be more pronounced until it starts to move through the upper nucleation size limit at which point the yield drops and the change in mean diameter is less marked. This accounts for the sigmoid profile of the mean diameter observed with pure Ni. Pure Co does not exhibit a sigmoid profile but shows almost no change in diameter (or yield) with temperature. As one adds increasing amounts of Co to Ni, the sigmoid profile becomes less pronounced and more spread out. This points to Co having a very broad precipitating cluster size distribution so that little change in temperature is observed. Hence, adding Co to Ni increases the precipitating cluster size distribution. This is reflected in the resultant SWNTs, which also have a broader size distribution (proportional to the fwhm). Adding Mo to Ni or Ni/Co also increases the precipitating cluster size distribution. Adding Mo to Co decreases the cluster size distribution. This is in agreement with the findings from Lolli *et al.*[10] All of the catalyst mixes have improved relative yields and have similar fwhm distributions (Figure 5). This process is illustrated in Figure 6, in which the fwhm data are also provided to help illustrate the process. In effect, the role of mixed catalysts is to optimize the size distribution of catalyst particles so as to maximize the precipitating cluster size distribution lying within the nucleation window. This process can account for the yield variation between mixed catalyst systems despite having similar SWNT diameter distributions (fwhm).

It is worth noting that the catalyst volume to surface area model also depends on the carbon solubility in the catalyst cluster. Thus, one might expect the mean diameters from Ni, which has a lower carbon solubility to Co, to be larger than for Co. However, Co is susceptible to martensitic transformation, *viz.* C is trapped within. Hence, larger Co catalyst clusters are required to provide sufficient carbon for the nucleating hemispherical cap. This also explains why all of the Co alloys used form SWNTs with larger mean diameters than systems without Co.

The overall findings fit remarkably well within the catalyst volume to surface area model,[11] in which nucleation can be defined as the formation of a stable hemispherical cap as a cooling catalyst particle precipitates carbon. This suggests that growth occurs from a solidified catalyst particle. If so, then it is likely that carbon addition to a growing SWNT occurs through surface diffusion, as argued by Hofmann *et al.*[17] Further studies are required to better elucidate this point.

CONCLUSION

Systematic studies on binary and ternary catalysts based in Ni, Co, and Mo were conducted. The data reveal a close synergy between reactor temperature, yield, and crystallinaty of the produced SWNT. The mean diam-

eter of the SWNT varies according to both temperature and catalyst choice. All of the findings are fully described within a simple model in which the nucleating hemispherical cap formation window (due to catalyst cluster volume to surface area considerations) overlaps with the precipitating cluster size distribution. The cross-over degree between the two windows establishes the SWNT diameter distribution (and mean) and yield. This study reveals that the diameter size distributions (catalyst cluster and SWNT) are also dependent on catalyst choice. The mixing of catalysts alters the diameter distribution of the precipitating catalyst clusters, at the point of nucleation, such that the overlap with the hemispherical nucleation window is maximized leading to higher yields. The best yields are obtained with a ternary catalyst formed from Ni/Co/Mo (5:4:1).

EXPERIMENTAL SECTION

A furnace-based laser evaporation system was used to synthesize the SWNT. The reaction was driven by an Nd:YAG laser (λ = 1064 nm, power = 2.5 GW per pulse, pulse width = 8 ns). Furnace temperatures between 1050 and 1250 °C were explored. High purity catalyst material (>99.9%) was used throughout. The catalysts used were Ni, Co, and Mo. These were mixed with different ratios depending on the experiment in question. The catalysts were then mixed with spectroscopy grade graphite (>99.9% pure) and pressed in a 13 mm dye to form a 3 mm thick target. The total catalyst content was always 10 wt %. Nitrogen was used as the buffer gas. All experiments were performed at 1000 mbar and a flow rate of 0.4 slpm. The as-produced SWNTs were collected at the rear of the reactor on a copper coldfinger, which also provides a well-defined reaction stop point.

A Bruker 113V/88 spectrometer was used for optical absorption measurements between 0.35 and 2.35 eV with a spectral resolution of 0.25 eV. Raman spectroscopic measurements were achieved using a Thermo-Scientific SmartRaman DXR spectrometer (80 to 3000 cm^{-1}) using a 780 nm excitation laser. The morphology of the samples was investigated using transmission electron microscopy (TEM) on a FEI Tecnai T20 operating at 200 kV and scanning electron microscopy (SEM) using a JEOL JSM-6510 operating at 20 kV. Samples investigated through optical absorption spectroscopy were prepared by drop coating on KBr crystals. The KBr prepared samples were kept consistent by using equal concentrations of sample and acetone when preparing a dispersed sample for drop coating onto the KBr crystal. The film thickness and measurement area were also consistent for all samples. These films were floated off in distilled water and captured on standard Cu TEM grids for the TEM studies.

Acknowledgment. S.T. thanks Siemens for support under the Siemens Masters Program. A.B. thanks the EU for an MC fellowship from the European Network CARBIO, Contract MRTN-CT-2006-035616. I.I. thanks the DAAD for financial support. I.I. and G.C. acknowledge partial support from the European Union project CARDEQ under Contract No. IST- 021285-2. This work has been partially funded by the WCU (World Class University) program through the Korea Science and Engineering Foundation funded by the Ministry of Education, Science and Technology (Project No. R31-2008-000-10100-0). We are grateful to J. Förster, S. Leger, and R. Hübel for technical support.

Supporting Information Available: OAS and Raman spectra. This material is available free of charge *via* the Internet at http://pubs.acs.org.

REFERENCES AND NOTES

1. Bethune, D. S.; Klang, C. H.; de Vreis, M. S.; Gorman, G.; Savoy, R.; Vazquez, J.; Beyers, R. Cobalt-Catalysed Growth of Carbon Nanotubes with Single-Atomic-Layer Walls. *Nature* **1993**, *363*, 605.
2. Seraphin, S.; Zhuo, D. Single-Walled Nanotubes Produced at High Yield by Mixed Catalysts. *Appl. Phys. Lett.* **1994**, *64*, 2087.
3. Journet, C.; Maser, W. K.; Bernier, P.; Loiseau, A.; Lamydela-Chapelle, M.; Lefrant, S.; Deniard, P.; Lee, R.; Fischer, J. E. Large-Scale Production of Single-Walled Carbon Nanotubes by the Electric-Arc Technique. *Nature* **1997**, *388*, 756.
4. Saito, Y.; Tani, Y.; Miyagawa, N.; Mitsushima, K.; Kasuya, A.; Nishina, Y. High Yield of Single-Walled Carbon Nanotubes by Arc Disharge Using Rh−Pt Mixed Catalyst. *Chem. Phys. Lett.* **1998**, *294*, 593.
5. Thess, A.; Lee, R.; Nikolaev, P.; Dai, H.; Petit, P.; Robert, J.; Xu, C.; Lee, Y. H.; Kim, S. G.; Rinzler, A. G.; Colbert, D. T.; Scuseria, G. E.; Tománek, D.; Fischer, J. E.; Smalley, R. E. Crystalline Ropes of Metallic Carbon Nanotubes. *Science* **1996**, *273*, 483.
6. Christen, H. M.; Puretzky, A. A.; Cui, H.; Belay, K.; Fleming, P. H.; Goehegan, D. B.; Lowndes, D. H. Rapid Growth of Long, Vertically Aligned Carbon Nanotubes through Efficient Catalyst Optimization Using Metal Film Gradients. *Nano Lett.* **2004**, *4*, 1939.
7. Noda, S.; Sugime, H.; Osawa, T.; Tsuji, Y.; Chiashi, S.; Murakami, Y.; Maruyama, S. A Simple Combinatorial Method to Discover Co−Mo Binary Catalysts That Grow Vertically Aligned Single-Walled Carbon Nanotubes. *Carbon* **2006**, *44*, 1414.
8. Liao, X. Z.; Serquis, A.; Jia, Q. X.; Peterson, D. E.; Zhu, Y. T.; Xu, H. F. Effect of Catalyst Composition on Carbon Nanotubes Growth. *Appl. Phys. Lett.* **2003**, *82*, 2694.
9. Little, R. B. Mechanistic Aspects of Carbon Nanotube Nucleation and Growth. *J. Cluster Sci.* **2000**, *14*, 135.
10. Lolli, G.; Zhang, L.; Balzano, L.; Sakulchaicharoen, N.; Tan, Y.; Resasco, D. E. Tailoring (*n*,*m*) Structure of Single-Walled Carbon Nnanotubes by Modifying Reaction Conditions and the Nature of the Support of CoMo Catalysts. *J. Phys. Chem. B* **2006**, *110*, 2108.
11. Rümmeli, M. H.; Kramberger, C.; Löffler, M.; Jost, O.; Bystrzejewski, M.; Grüneis, A.; Gemming, T.; Pompe, W.; Büchner, B.; Pichler, T. Catalyst Volume to Surface Area Constraints for Nucleating Carbon Nanotubes. *J. Phys. Chem. B* **2007**, *111*, 8234.
12. Itkis, M. E.; Perea, D.; Jung, R.; Niyogi, S.; Haddon, R. C. Comparison of Analytical Techniques for Purity Evaluation of Single-Walled Carbon Nanotubes. *J. Am. Chem. Soc.* **2005**, *127*, 3439.
13. Rümmeli, M. H.; Borowiak-Palen, E.; Gemming, T.; Pichler, T.; Knupfer, M.; Kalbac, M.; Dunsch, L.; Jost, O.; Silva, S. R. P.; Pompe, W.; Büchner, B. Novel Catalysts, Room Temperature, and the Importance of Oxygen for the Synthesis of Single-Walled Carbon Nanotubes. *Nano Lett.* **2005**, *5*, 1209.
14. Bystrzejewski, M.; Schönfelder, R.; Cuniberti, G.; Lange, H.; Huczko, A.; Gemming, T.; Pichler, T.; Büchner, B.; Rümmeli, M. H. Exposing Multiple Roles of H_2O in High-Temperature Enhanced Carbon Nanotube Synthesis. *Chem. Mater.* **2008**, *20*, 6586.
15. Liu, X.; Pichler, T.; Knupfer, M.; Golden, M. S.; Fink, J.; Kataura, H.; Achiba, Y. Detailed Analysis of the Mean Diameter and Diameter Distribution of Single-Wall Carbon Nanotubes from Their Optical Response. *Phys. Rev. B* **2002**, *66*, 45411.
16. Fan, X.; Buczko, R.; Puretzky, A. A.; Geohegan, D. B.; Howe, J. Y.; Pantelides, S. T.; Pennycook, S. J. Nucleation of Single-Walled Carbon Nanotubes. *Phys. Rev. Lett.* **2003**, *90*, 145501.
17. Hofmann, S.; Csányi, G.; Ferrari, A. C.; Payne, M. C.; Robertson, J. Surface Diffusion: The Low Activation Energy Path for Nanotube Growth. *Phys. Rev. Lett.* **2005**, *95*, 036101.